2D Seismic Data Classification using Convolutional Neural Network and 2D Synthetic Data

Alice Y. Yang, Musa Manzi, Michael Westgate, and Ling Cheng

Johannesburg, South Africa

Abstract

The following paper looks at classifying 2-dimensional seismic data extracted from South African geo-location using a Convolutional Neural Network (CNN) that is trained with synthetic data. The purpose of this paper illustrates the difficulties in working with seismic data and the precision needed for automating feature extraction within the CNN architecture in order to achieve a 90%. The CNN architecture is mainly constructed using 2D convolutional and max-pooling layers.

Keywords: 2D Seismic Data, Convolutional Neural Network, Synthetic Data

1. Introduction

In the recent years, Artificial Intelligence (AI) has grew exponentially and is applied to various disciplines and it is no surprise that it has found its way into amongst geologist in the geology field. Given that geologist work with large quantities of geological data to map both the surface of the earth and the mapping of faults below the surface, there is an enormous data and potential for AI. The traditional method of interrupting subsurface data includes manual fault picking and horizons on section, which is then followed by qualitative enhancements [1]. The qualitative enhancement techniques involves structurally-oriented semblance, tensor, dip, and etc. for highlighting the fault structure within the subsurface seismic dataset [1].

This paper addresses alternative approaches for classifying seismic data using Artificial Intelligence and more specifically, using the Convolutional Neural Network (CNN) for classifying 2D seismic image data. The objective of the purposed technique is to detect whether there is intersecting fault or

none-intersecting within 2D seismic data. The paper is structured in such a manner where Section 2 gives a brief background of the techniques used in the proposed technique. Section 4 describes the methodology and the process of achieving the results addressed in Section 5 before finally concluding in Section 7.

2. Background

2.1. Convolutional Neural Network

The Convolutional Neural Network (CNN) is a subsidiary of supervised technique within in the deep learning field. It is commonly employed for image classification purposes due to its exceptional ability to purpose image analysis using the mathematical convolutional operation and obtaining high classification accuracies [2, 3]. Due to the CNN's high classification accuracy, it has been utilised within multiple fields including the geological realm for earthquake detection and location [4], seismic inversions [5], and fault detection [6, 7].

Given that the CNN is a supervised neural network, it learns images features based in order to form an end-to-end model with the trained parameters through the gradient descent method. Therefore, the CNN model makes use of connected weights within the network as a form of sharing "knowledge" and reducing the number of training parameters, and as a result also reducing redundant complexity [3, 8]. In general, the first few layers of the CNN architecture consists of convolution and pooling layers, whilst the layers following there after are fully-connected network [3, 9].

The training of the CNN is conducted mainly using both back- and forward propagation algorithms to adjust the weights of the neurons based on the given training data. The objective of the back-propagation algorithm is to adjust the weights to minimise loss based on the network's overall outcome and the target. The network's overall outcome is obtained using the forward propagation. The back-propagation loss function, $E(W, b)$ is expressed in (1) as the Mean Squared Error (MSE).

$$E(W, b) = \frac{1}{|Y|} \sum_{i=1}^{|Y|} (Y(i) - \bar{Y}(i)^2), \tag{1}$$

where W is the weight value and b is the b is the bias value. Both the weight value, W and bias value, b are updated during the back-propagation training

according to (2) and (3), respectively.

$$W_i = W_i - \eta \frac{\partial E(W, b)}{\partial W_i} \tag{2}$$

$$b_i = b_i - \eta \frac{\partial E(W, b)}{\partial b_i}, \tag{3}$$

where η is the learning rate.

3. Literature Review

Wu, X. et al.performed image-to-image binary fault detection using a fully-supervised CNN [6]. The authors made use of 3D seismic images which where labelled with ones for fault and zeros elsewhere. The CNN model was trained with 200 3D synthetic seismic images with a $128 \times 128 \times 128$ dimension for each fault and non-fault category. The training of the neural network was performed on a TITAN Xp GPU which took the authors approximately 2 hours to train. The authors validated the network with 20 pairs of unseen synthetic image data, in which the network achieved a 95% classification accuracy. The generated synthetic data consists of faults at varying angles, specially at 90°, 180°, and 270°. Additionally, the authors applied the trained CNN to detect faults on surveyed 3D data from four different locations, namely the Netherlands off-shore data, Clyde Petroleum Plc., Costa Rica margin North West of Osa Peninsula, and Campos Basin which is off-shore of Brazil.

Zheng, Y. et al. presents two separate case studies involving supervised deep learning as an alternative for the conventional techniques in seismic data interpretation and inversion [10]. In the first case study, the authors apply the CNN for seismic image classification as a way of interpretation. The CNN is trained with 3D seismic volumes, such that images are classified into two categories, namely, fault and non-fault. The fault data consists of certain dips as well as azimuth, which are distinguishing features in the data considered as faults. In the second case study, the authors present an elastic model building, in which a CNN is trained to perform predictions of 1D velocity and density profiles within the given seismic data. In both case studies, the authors have trained the CNN models using synthetic data and tested the models on survey field data. The authors have found that both CNN models obtained effective and efficient predictions when testing

on field data, therefore showing high-quality fault picks. However, challenges are presented when the authors worked with pre-stacked seismic inversions, where subsurface geological variations and preconditioning of the input seismic data plays an important factor in the ability of the CNN models to perform accurate predictions.

The author, Zhao, T. presents an encoder-decoder CNN model for seismic facies classification [11]. The architecture of the encoder-decoder CNN model consists of an encoding component, in which the input data given to the model is reduced and a decoding component, whereby the reduced data is then expanded once again. The purpose of the encoding component is to reduce the input data such that only the significant portions of the input data is kept, whilst the decoding component further highlights and expands on the significant data such that contributing noise within the input data is removed. This allows for enhanced fault predictions in seismic faces. Additionally, the author has compared the presented CNN model to the architecture of the more traditional patch-base CNN model, in which the author found that the patch-base CNN model requires less training effort compared to the encoder-decoder CNN model, however the patch-based CNN produced suboptimal predictions compared to the encoder-decoder CNN.

Di, H et al. introduces a CNN model for the application of salt-body delineation from 3D seismic data [12]. The authors have found the implementation of the CNN model is far more superior when compared to the traditional schemes of sample-based multi-attribute classification. The implemented CNN model takes the local seismic patterns which are distinguishing features within the target salt-body. Furthermore the CNN allows for optimal mapping relationship between the seismic signals and the salt-bodies, and as a result it does not require laborious manual attribute selection as performed in the traditional classification schemes. The CNN model was trained using synthetic data from the SEG-SEAM dataset.

Xiong, W. et al. developed a method which employs the CNN to automate and map fault detection in 3D seismic images to mimic the traditional approach by interpretors. The CNN is trained with image cubes obtained from field data which are labelled as either fault or non-fault. The trained CNN is then applied to unseen field data to predict the fault probabilities at every location with given cube images. The authors have been able to obtain a 99% classification accuracy using the trained CNN.

4. Methodology

The technique consists of two processes. The first process is training the CNN and the second is applying the trained CNN to unseen 2D seismic data extracted from South African geological sub-surfaces. The two processes are illustrated in Figure 1, in which the training process is depicted on the left and the testing process on the right.

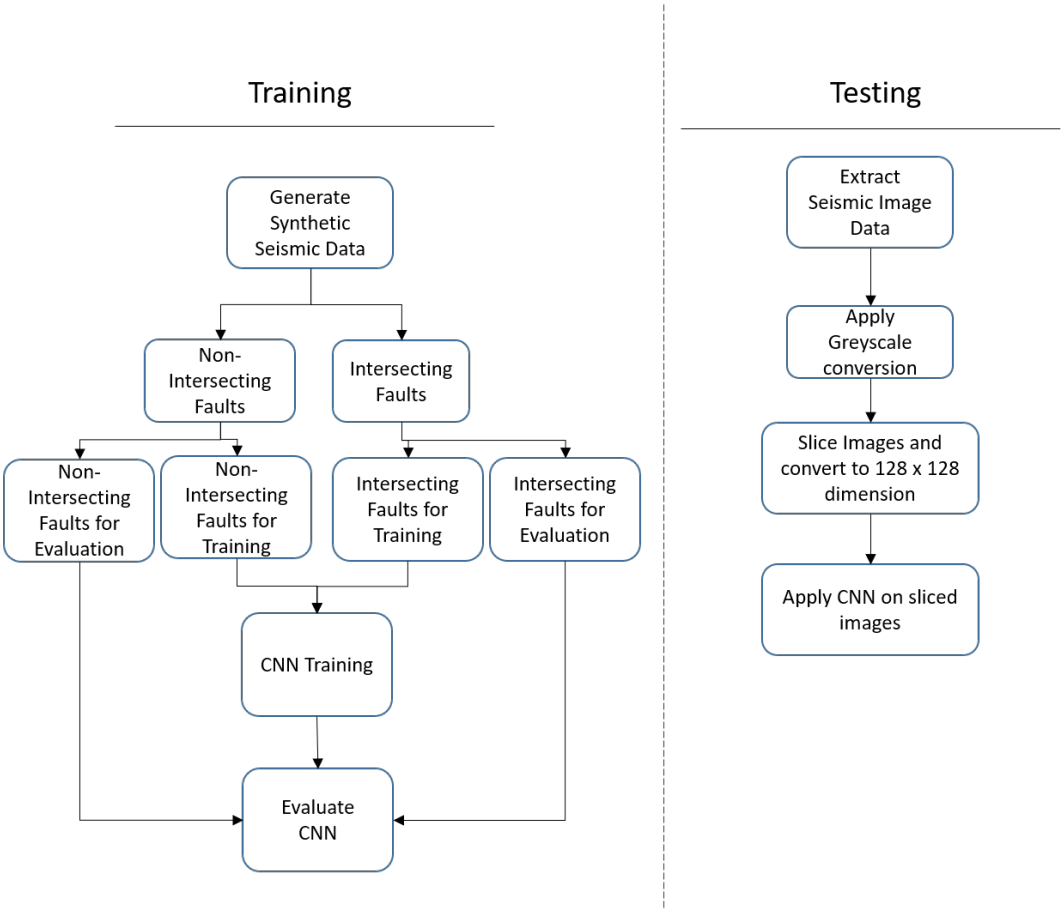

Figure 1: Diagrams illustrating the training and testing processes involving the Convolutional Neural Network.

4.1. Training Images

The data used for training the CNN is taken from https://github.com/xinwucwp/faultSeg, whereby the data is given as 3D $128 \times 128 \times 128$

seismic data, which is generated by Wu, X. et al [6]. The data is transformed from 3D to 2D, by taking slices of the 3D block to generate 2D 128×128 seismic data. From the synthetic data, only the seismic data which has intersecting and none-intersecting faults are selected. Figures in 2 and 3 illustrates the training data. Both images 2(b) and 3(b) are not used as part of the training data, however are used to assist in the labelling of intersecting and non-intersecting fault data. A total of 350 seismuc images are used in each category for the training of the CNN.

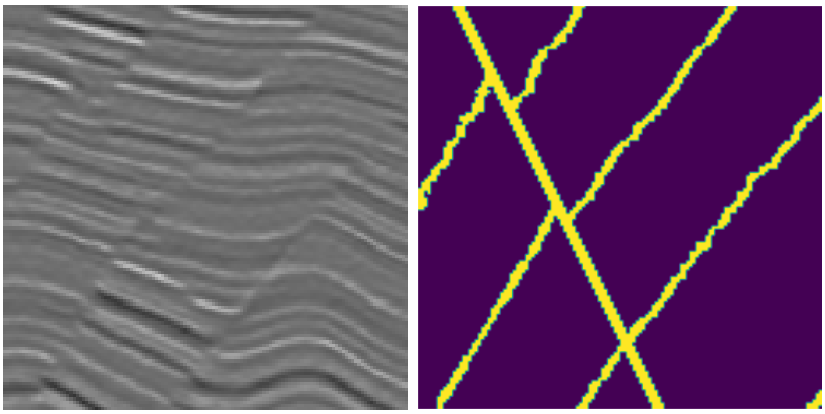

(a) Seismic Image with Intersecting Fault

(b) Hightlighted Intersecting Fault in Seismic Image

Figure 2: Images illustrating the Intersecting Seismic Data and Highlighted Faults in the Seismic image.

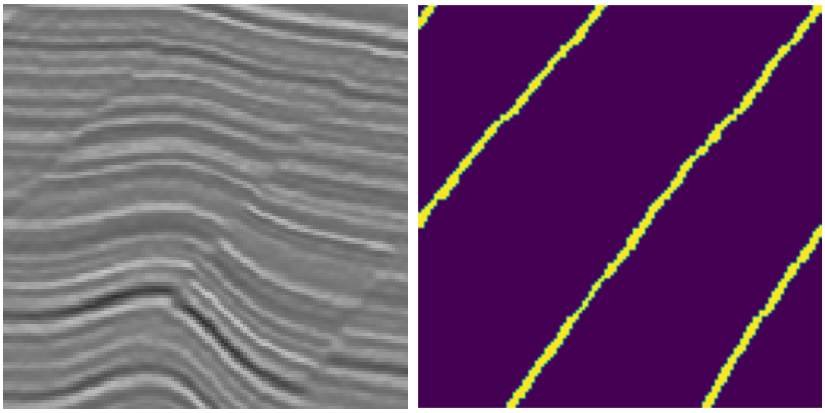

(a) Seismic Image with Non-Intersecting Fault

(b) Hightlighted Non-Intersecting Fault in Seismic Image

Figure 3: Images illustrating the Non-Intersecting Seismic Data and Highlighted Faults in the Seismic image.

4.2. Convolutional Neural Network Architecture

The CNN is comprised of three distinct layers excluding the input and output layer, namely 2D convolutional, max pooling and fully connected layers. There are a total of four hidden layers in the neural network architecture. The 2D convolutional layer makes use of the Rectified Linear Unit (Relu) function. Figure 4 shows the detailed architecture of CNN. The CNN is trained with 25 epochs. Figure 5 shows the accuracy and validation accuracy of the CNN at each epoch.

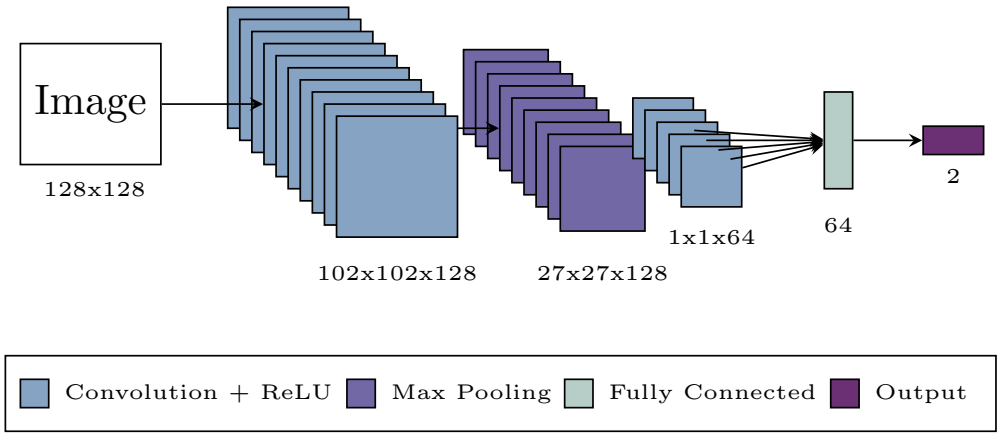

Figure 4: Figure illustrating the architecture of the Convolutional Neural Network

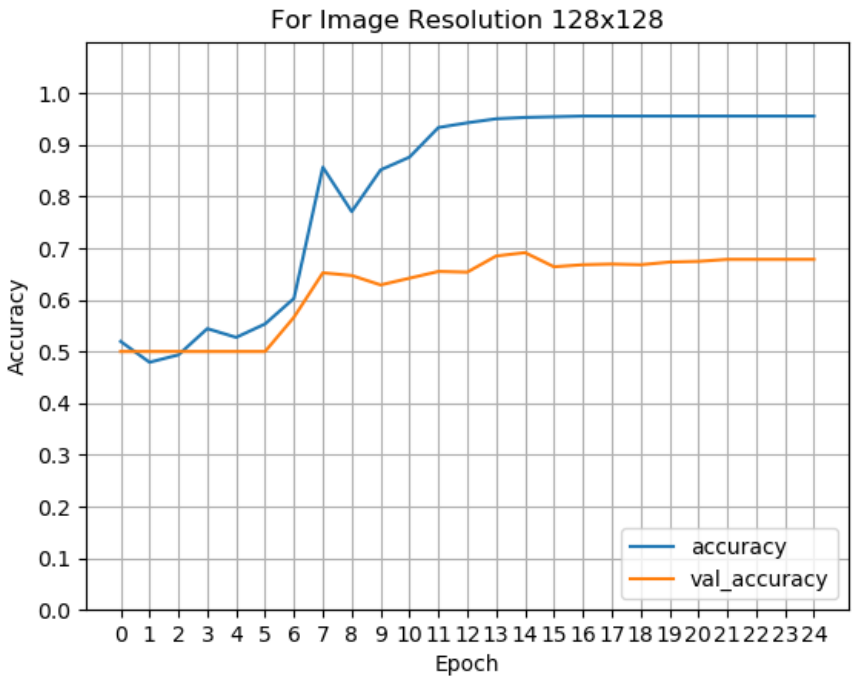

Figure 5: Figure illustrating accuracy of the CNN at each epoch

4.3. Seismic Data Testing

The seismic testing data consists of surface and edge detected images of the orebody. The two image considered as shown in Figures 6 and 7, in which both images are taken from a South African gold mine.

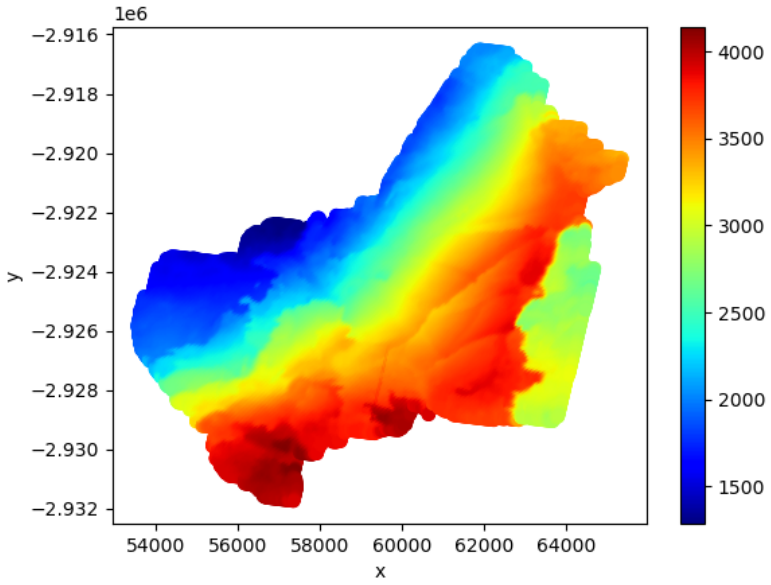

Figure 6: Figure illustrating the orebody surface extracted from a gold mine.

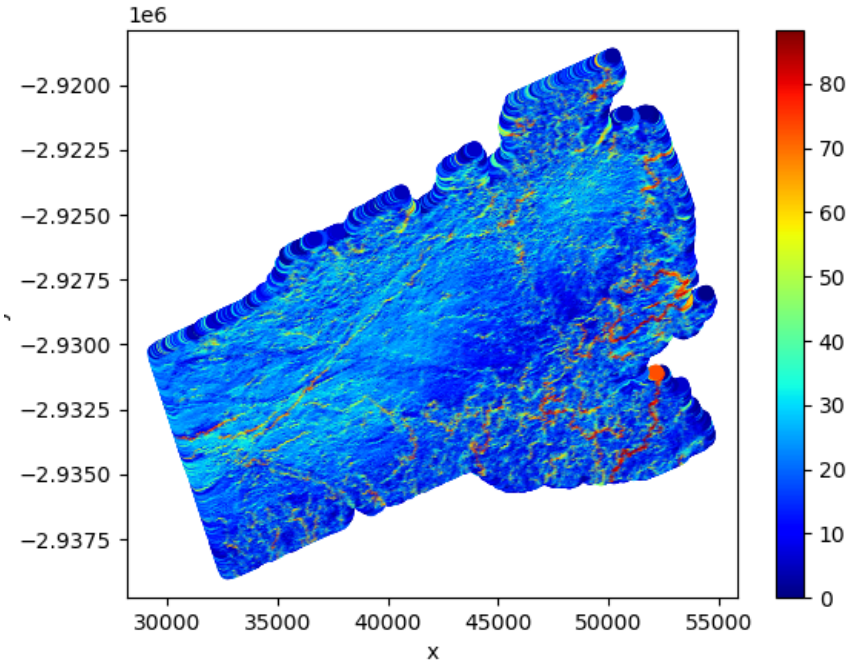

Figure 7: Figure illustrating the orebody surface with highlighted edges extracted from a gold mine.

Figure 7 has been further processed in order for the fault edges to be highlighted. A closer and more detailed illustration of of both Figures 6 and 7 are shown in Figures 12(a) and 12(b). The detailed images are generated through the process of slicing the original seismic image data. The process is illustrated in Figure 10, whereby the process consists of converting the original image into greyscale, followed by slicing the images into equal segments before finally resizing the segmented images to images with the dimensions of 128×128, using the k-nearest neighbour method. In addition to the gold mine image data, image data taken from oil and gas mines are considered when testing the CNN model, which is illustrated in Figure 13.

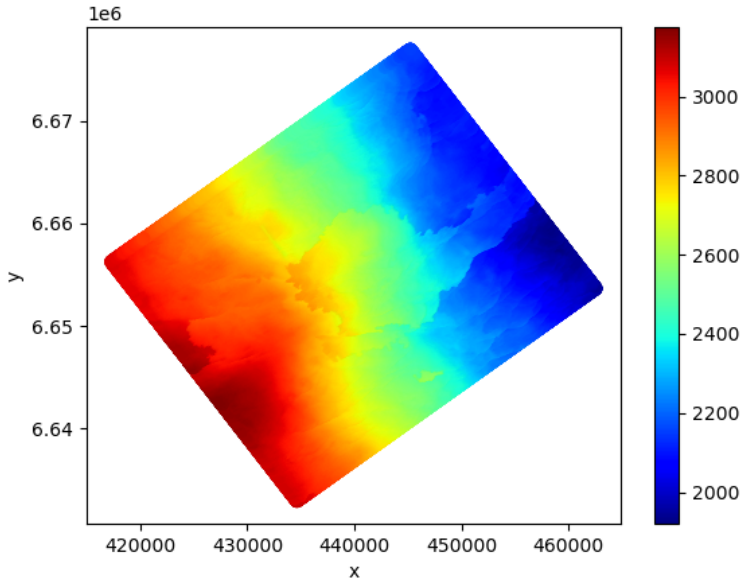

Figure 8: Figure illustrating the orebody surface extracted from an oil and gas mine.

5. Results

The segmented images from the different mines are fed into the CNN. The results of the CNN are shown in the following section for the datasets from gold, and oil and gas mines. Figures 15 and 16 illustrates the classification of crossing faults ("x") and none-crossing faults ("none-x") are present in the surface orebody image and highlighted edge image, respectively.

The result of the CNN for Figure 15 indicates that the CNN has classified the surface image data as being an image with crossing faults based in the training of the CNN, in which the classification is based on a 53% assurance. This shows that CNN identifies 47% of none-crossing faults within the given image. However since there are more crossing faults presented, the image is classified in the category of having crossing faults.

Figure 16 shows the result of the CNN for highlighted edges for data taken in a gold mine. With the highlighted edges the CNN can distinctively identify with 99% confidence that the image is categorised as having crossing faults, whilst there is still a 1% chance that there is non-crossing faults within the section of data.

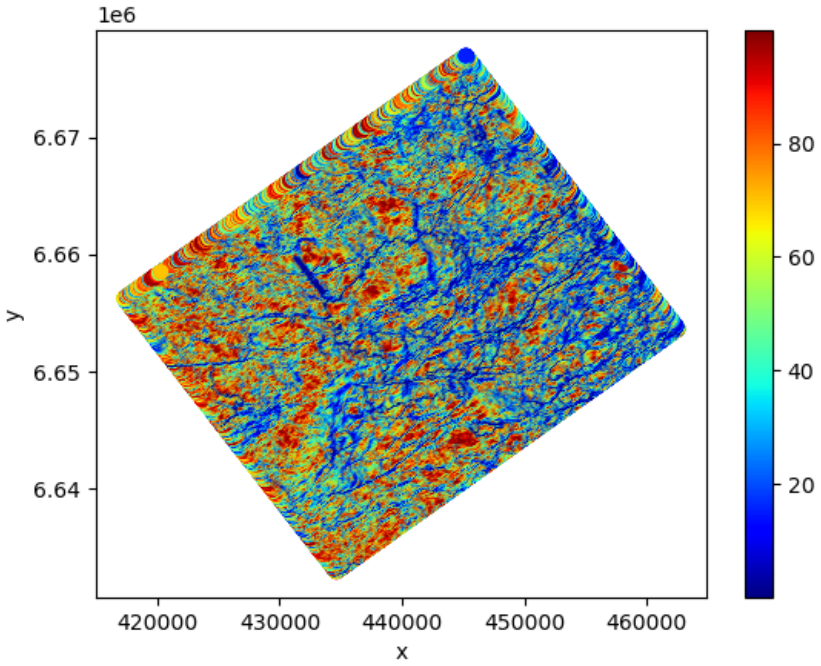

Figure 9: Figure illustrating the orebody surface with highlighted edges extracted from an oil and gas.

For the surface data taken from oil and gas mines, Figure 17 shows that the CNN has a 71% confidence in classifying the given image as having none-crossing faults, whilst having a 29% chance of having crossing faults within the image. These crossing faults are difficult to identify with the naked eye. However, it is presented in the bottom right corner within the image.

The classification of the highlighted edge image for the gas and oil mine data is similar to that of the gold mine shown in Figure 18. The CNN is 97% confident in classifying the given image as having crossing faults.

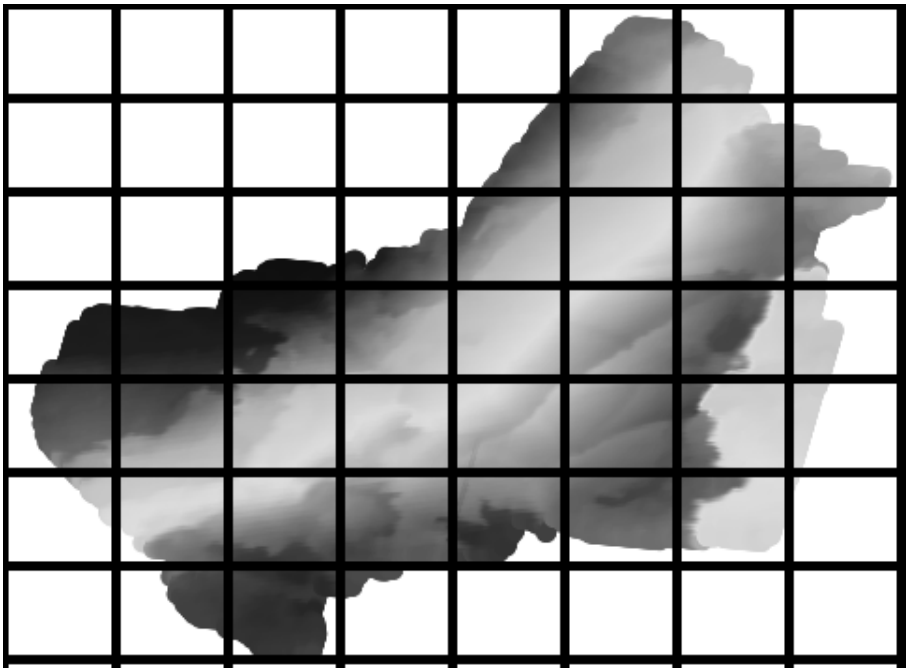

Figure 10: Slicing process of gold mine seismic image data for Figure 6.

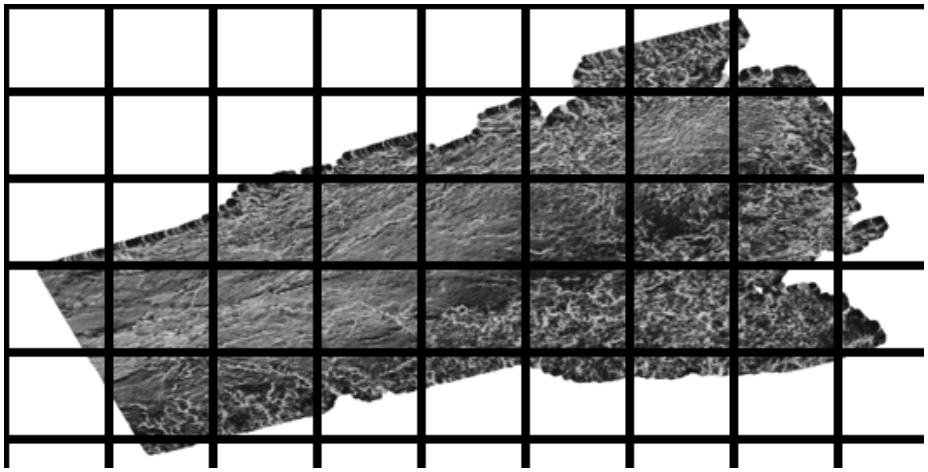

Figure 11: Slicing process of gold mine seismic image data for Figure 6.

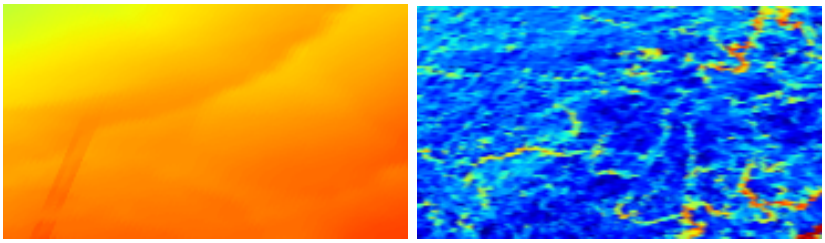

(a) Surface Seismic Data (b) Hightlighted Edge Surface Data

Figure 12: Images illustrating both seismic orebody surface and highlighted edge surface data taken from two different gold mines.

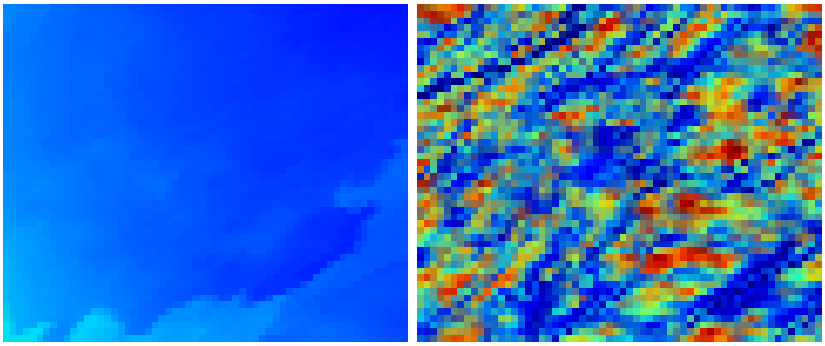

(a) Surface Seismic Data (b) Hightlighted Edge Surface Data

Figure 13: Images illustrating both seismic orebody surface and highlighted edge surface data taken from an oil and gas mine.

6. Application

The results of the CNN in the classification of images with crossing and non-crossing faults are promising as discussed in Section 5. Therefore, the CNN can be applied to a set of data, in which it the areas of the image are segmented into a number of images. This is illustrated in Figure 19. The segmented images are then fed into the CNN to determine areas that consist of a high density of intersecting faults, whilst all background images that holds little to no information about the image data are disregarded.

The process depicted in Figure 19 is applied to the Figure 6 to determine the density of intersecting faults within the seismic data. The density of intersecting faults is measured by the confidence level of the CNN in its

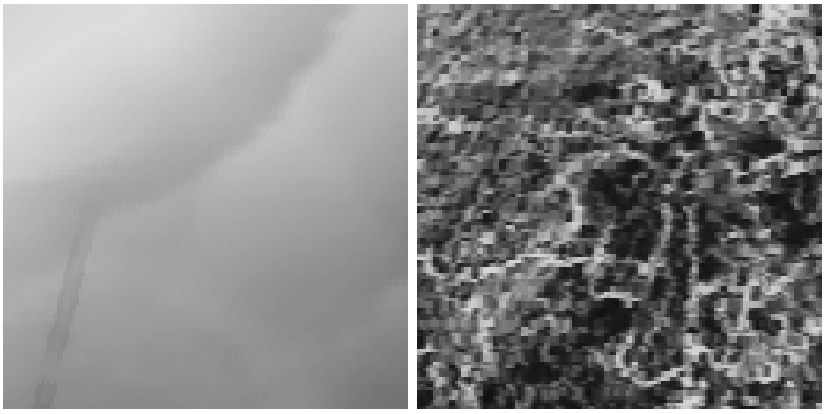

(a) Processed Surface Seismic Data of 14(a)

(b) Processed Hightlighted Edge Surface Data of 13(b)

Figure 14: Images illustrating both the processed seismic orebody surface and highlighted edge surface data.

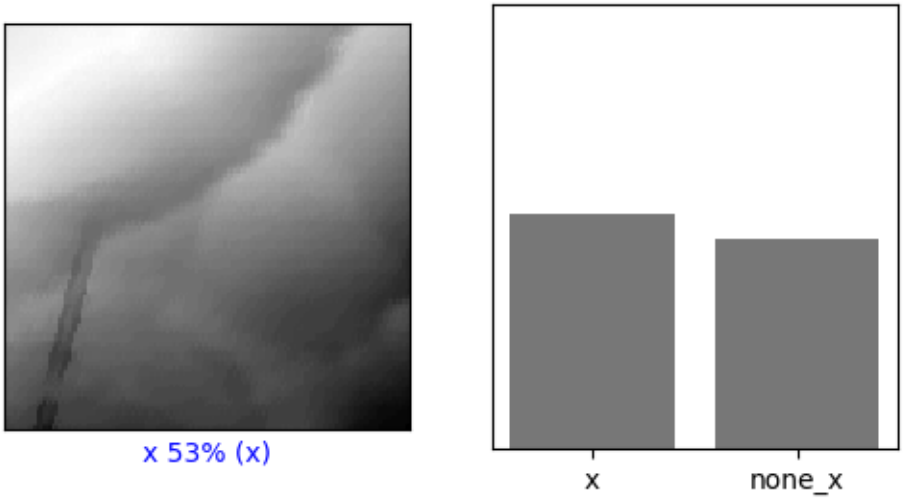

Figure 15: Figure illustrating the CNN classification result of Figure 14(a)

prediction of whether the segmented image is classified into the intersecting and non-intersecting fault categories. The measurement is based on the training of the CNN model, therefore a higher confidence in category predic-

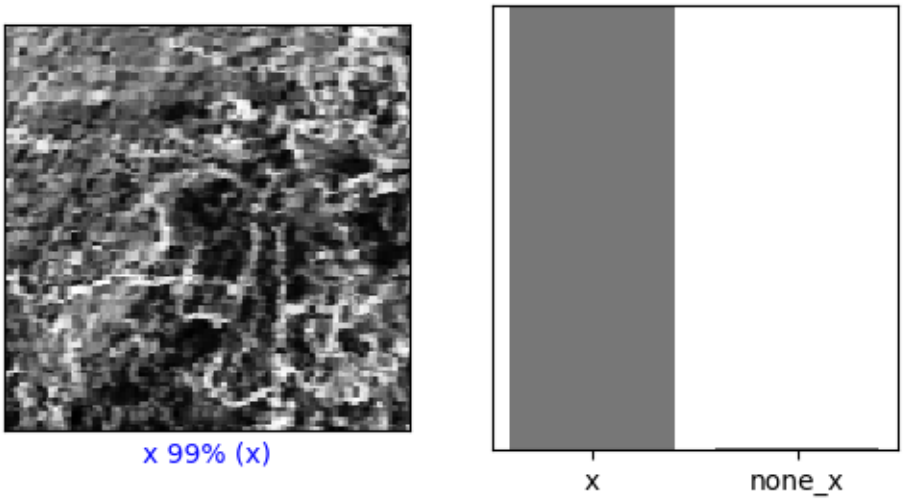

Figure 16: Figure illustrating the CNN classification result of Figure 14(b)

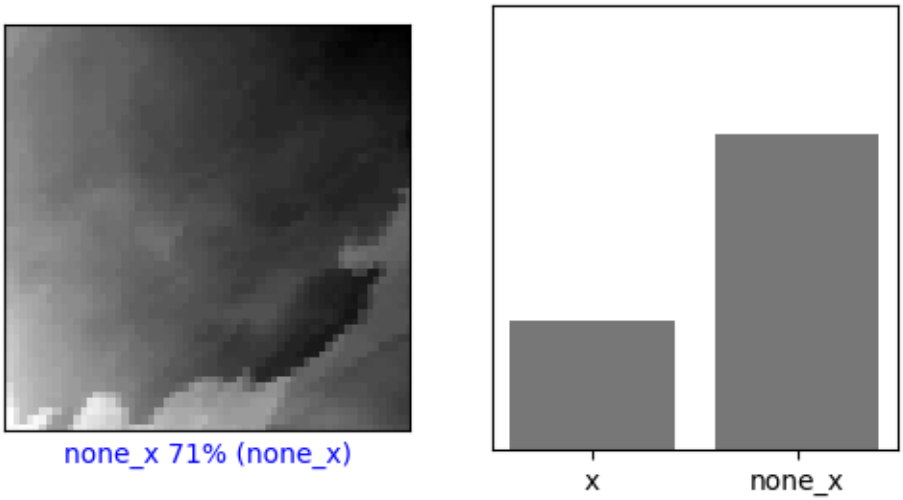

Figure 17: Figure illustrating the CNN classification result of Figure **??**

tion shows that there is a higher likelihood of high density of the predicted category. The prediction results shown in Figure 20 indicate that there is a

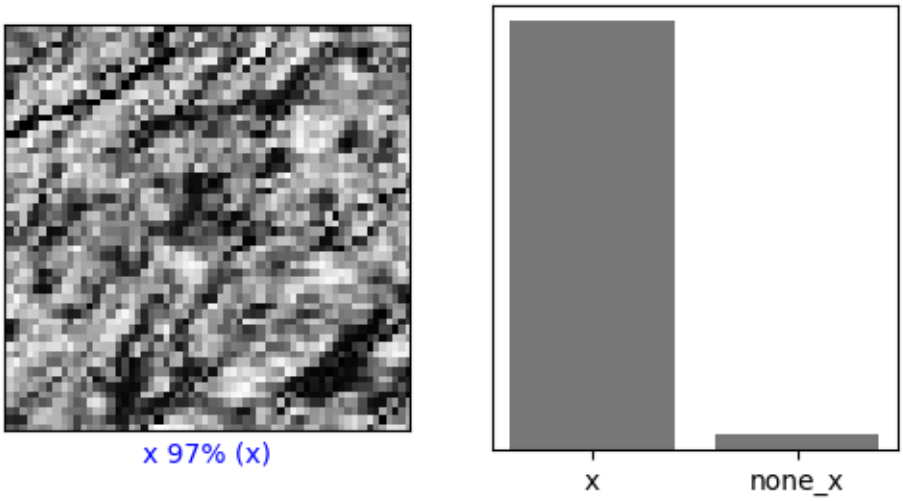

Figure 18: Figure illustrating the CNN classification result of Figure **??**

low density of intersecting faults in majority of the surface image segments of Figure 6, whilst there is a single segment with 81% confidence for classifying the image segment in the intersecting fault category.

The results shown in Figure 21 is generated from Figure 7. The results show more certainty in classification by the CNN in comparison to the results shown in Figure 20. Therefore, with the highlighted edges provides additional information to the CNN model for classification purposes. However, it must be noted that the texture of within Figure 7 is similar to the training images used in the training of the CNN, in which this is a contributing factor to the increased decisiveness in categorising the image segments into intersecting and non-intersecting categories. Whereas, the texture in Figure 6 has a smooth texture in comparison to Figure 7, therefore the results presented show a more indecisive prediction in the 50% to 60% range.

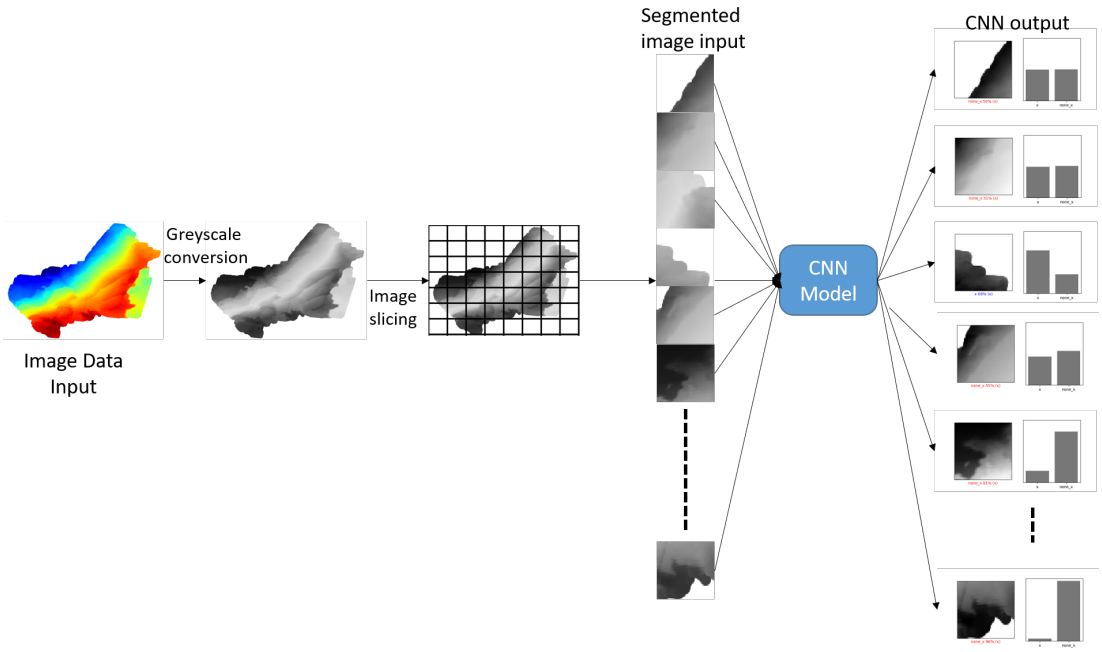

Figure 19: Diagram showing the process in the application of the CNN model. The diagram includes the processing of the seismic image data.

7. Conclusion

References

[1] J. Lowell, P. Szafian, N. Tessen, Artificial Intelligence and Seismic Interpretation, GEO ExPro (2019). URL: http://www.geoexpro.com/articles/2019/05/artificial-intelligence-and-seismic-interpretation.

[2] A. Krizhevsky, I. Sutskever, G. E. Hinton, Imagenet classification with deep convolutional neural networks, Communications of the ACM 60 (2017) 84–90.

[3] W. Zhiqiang, L. Jun, A review of object detection based on convolutional neural network, in: 2017 36th Chinese Control Conference (CCC), IEEE, 2017, pp. 11104–11109.

[4] T. Perol, M. Gharbi, M. Denolle, Convolutional neural network for earthquake detection and location, Science Advances 4 (2018) e1700578.

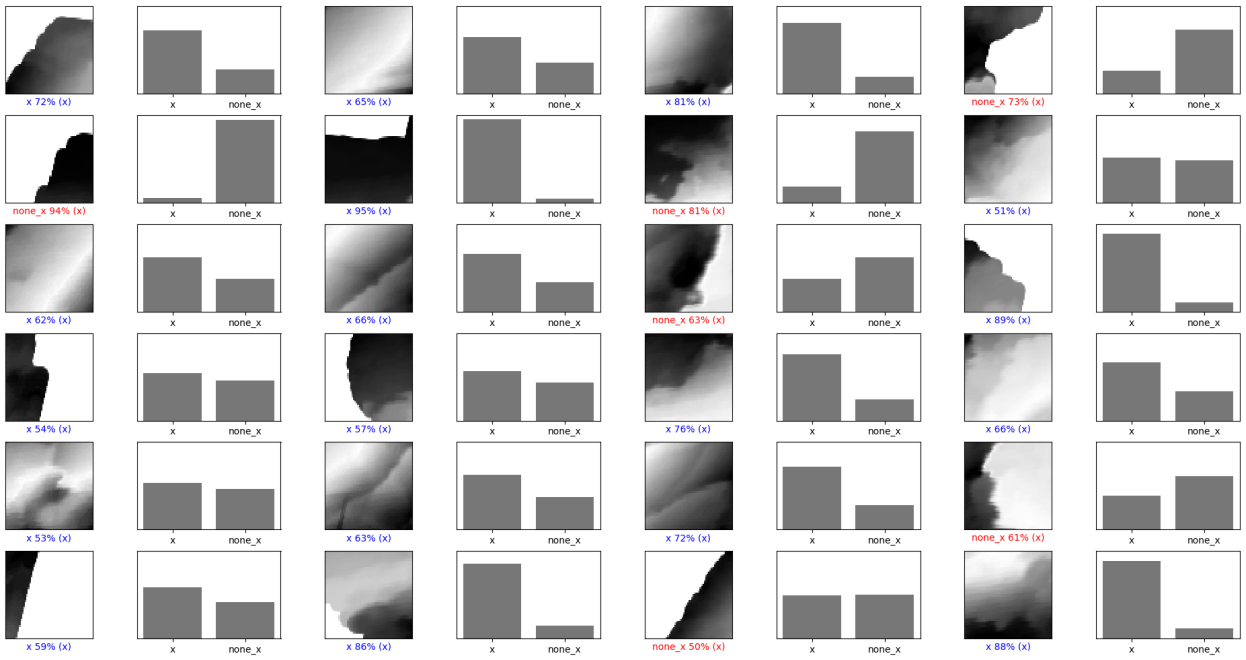

Figure 20: Figure illustrating region classification for the crossing fault detection for gold mine orebody surface.

[5] V. Das, A. Pollack, U. Wollner, T. Mukerji, Convolutional neural network for seismic impedance inversion, in: SEG Technical Program Expanded Abstracts 2018, Society of Exploration Geophysicists, 2018, pp. 2071–2075.

[6] X. Wu, L. Liang, Y. Shi, S. Fomel, Faultseg3d: Using synthetic data sets to train an end-to-end convolutional neural network for 3d seismic fault segmentation, Geophysics 84 (2019) IM35–IM45.

[7] W. Xiong, X. Ji, Y. Ma, Y. Wang, N. M. AlBinHassan, M. N. Ali, Y. Luo, Seismic fault detection with convolutional neural network, Geophysics 83 (2018) O97–O103.

[8] N. Chumerin, Convolutional neural network, Neurocomputing 148 (2015) 136–142.

[9] Y. LeCun, L. Bottou, Y. Bengio, P. Haffner, Gradient-based learning

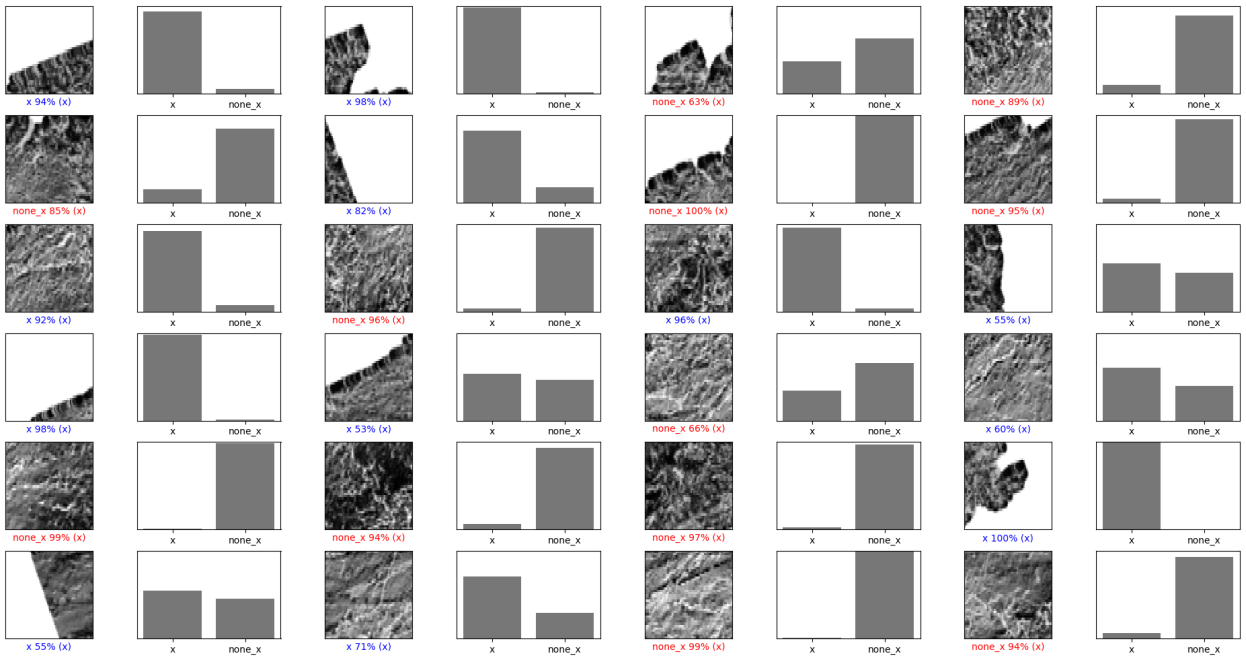

Figure 21: Figure illustrating region classification for crossing fault detection for the gold mine edge image data

applied to document recognition, Proceedings of the IEEE 86 (1998) 2278–2324.

[10] Y. Zheng, Q. Zhang, A. Yusifov, Y. Shi, Applications of supervised deep learning for seismic interpretation and inversion, The Leading Edge 38 (2019) 526–533.

[11] T. Zhao, Seismic facies classification using different deep convolutional neural networks, in: SEG Technical Program Expanded Abstracts 2018, Society of Exploration Geophysicists, 2018, pp. 2046–2050.

[12] H. Di, Z. Wang, G. AlRegib, Deep convolutional neural networks for seismic salt-body delineation, in: AAPG Annual Convention and Exhibition, 2018.